Chemosphere 356 (2024) 141780

Contents lists available at ScienceDirect

Chemosphere

journal homepage: www.elsevier.com/locate/chemosphere

Degradation and mineralization of anti-cancer drugs Capecitabine, Bicalutamide and Irinotecan by UV-irradiation and ozone

Stephan Zimmermann [a], Messika Revel [b], Ewa Borowska [a], Harald Horn [a,c,*]

[a] Karlsruhe Institute of Technology (KIT), Engler-Bunte-Institut, Water Chemistry and Water Technology, Engler-Bunte-Ring 9, 76131, Karlsruhe, Germany
[b] UniLaSalle - Ecole des Métiers de L'Environnement, CYCLANN, Campus de Ker Lann, F-35170, Bruz, France
[c] DVGW Research Laboratories for Water Chemistry and Water Technology, Engler-Bunte-Ring 9, 76131, Karlsruhe, Germany

HIGHLIGHTS

- Degradation of three anti-cancer drugs by ozonation and UV-irradiation was shown.
- Capecitabine, Bicalutamide and Irinotecan are all degradable by UV-irradiation.
- Capecitabine and Irinotecan, but not Bicalutamide, are susceptible to direct ozonation.
- Rate constants for ozonation and quantum yields of photolysis were calculated.
- Mineralization was low during ozonation, but up to 80% during UV-irradiation.

GRAPHICAL ABSTRACT

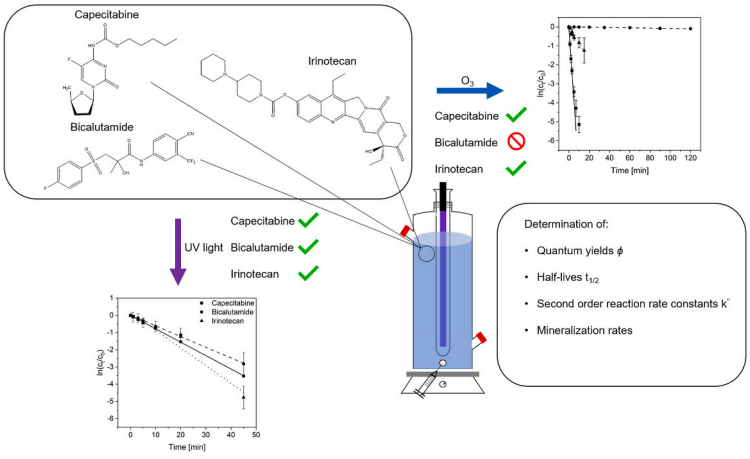

ARTICLE INFO

Handling Editor: Jun Huang

Keywords:
Anti-cancer drugs
Ozonation
UV
Mineralization
Degradation kinetics

ABSTRACT

The degradation of three anti-cancer drugs (ADs), Capecitabine (CAP), Bicalutamide (BIC) and Irinotecan (IRI), in ultrapure water by ozonation and UV-irradiation was tested in a bench-scale reactor and AD concentrations were measured through ultra-high-performance liquid chromatography tandem mass spectrometry (UHPLC-MS/MS). A low-pressure mercury UV (LP-UV) lamp was used and degradation by UV ($\lambda = 254$ nm) followed pseudo-first order kinetics. Incident radiation in the reactor was measured via chemical actinometry using uridine. The quantum yields (φ) for the degradation of CAP, BIC and IRI were 0.012, 0.0020 and 0.0045 mol Einstein^{-1}, respectively. Ozone experiments with CAP and IRI were conducted by adding ozone stock solution to the reactor either with or without addition of tert-butanol (t-BuOH) as radical quencher. Using this experimental arrangement, no degradation of BIC was observed, so a semi-batch setup was employed for the ozone degradation experiments of BIC. Without t-BuOH, apparent second order reaction rate constants for the reaction of the ADs with molecular ozone were determined to be 3.5 ± 0.8 • 10^3 L mol^{-1} s^{-1} (CAP), 7.9 ± 2.1 • 10^{-1} L mol^{-1} s^{-1} (BIC)

* Corresponding author. Karlsruhe Institute of Technology (KIT), Engler-Bunte-Institut, Water Chemistry and Water Technology, Engler-Bunte-Ring 9, 76131 Karlsruhe, Germany.
E-mail address: harald.horn@kit.edu (H. Horn).

https://doi.org/10.1016/j.chemosphere.2024.141780
Received 12 October 2023; Received in revised form 26 February 2024; Accepted 22 March 2024
Available online 9 April 2024

and $1.0 \pm 0.3 \bullet 10^3$ L mol^{-1} s^{-1} (IRI). When OH-radicals (•OH) were quenched, rate constants were virtually the same for CAP and IRI. For BIC, a significantly lower constant of $1.0 \pm 0.5 \bullet 10^{-1}$ L mol^{-1} s^{-1} was determined. Of the tested substances, BIC was the most recalcitrant, with the slowest degradation during both ozonation and UV-irradiation. The extent of mineralization was also determined for both processes. UV irradiation was able to fully degrade up to 80% of DOC, ozonation up to 30%. Toxicity tests with *Daphnia magna* (*D. magna*) did not find toxicity for fully degraded solutions of the three ADs at environmentally relevant concentrations.

1. Introduction

Cancer was the leading cause of death for people below the age of 70 in 48 countries and the second leading cause in another 43 countries in 2015 (Bray et al., 2018). The cancer incidence is expected to increase by more than 50% until 2040 (International Agency for Research on Cancer, 2020). This increase is caused by multiple factors including growing and ageing populations. After diagnosis, some of the main treatment methods are surgery, radiation therapy or administration of ADs during chemotherapy. Often, these therapies are combined. With an increase in the number of cancer patients, the amount of administered ADs is likely to increase as well.

Like other pharmaceuticals, ADs are partly transformed in the body while parts are excreted unchanged via urine or faeces and end up in waste water treatment plants (WWTPs). According to a study by (Besse et al., 2012), only 14% of ADs in France are administered at the hospital, while the majority is consumed in practical offices or at home. Some ADs are resistant to complete degradation in WWTPs and from those that reach the WWTP, a substantial amount is released into the environment (Gouveia et al., 2020). Concentrations of ADs in the environment are typically in the range of ng L^{-1}, but despite these low concentrations it has been shown that some substances potentially pose an environmental risk at concentrations present in surface waters because of their high toxicity (Mišík et al., 2019).

Ozonation and irradiation by UV light are processes that have been shown to be able to degrade micropollutants in general, and ADs in specific in water (Garcia-Costa et al., 2021). By adding a fourth treatment step to WWTPs, the concentration of harmful substances in WWTP effluent can be reduced, which is why Switzerland decided to finally upgrade 100 of its biggest WWTPs with a fourth clean-up step until 2035 (Der Bundesrat, 2023).

During ozonation, ozone dissolves in the water and reacts with substances dissolved in water, including ADs. Ozone can degrade substances in two ways, by reacting directly or indirectly. Direct ozone reactions refer to the reaction of ozone with specific moieties of pollutants, like aromatics, olefins and amines. In water, especially when the pH value is elevated, ozone also produces hydroxyl radicals (•OH), which are highly reactive and less selective than ozone. This is called indirect ozonation, because ozone does not react directly with the degraded compounds. In the presence of •OH, higher mineralization of organic compounds can therefore be achieved when compared to ozone alone (Sonntag and Gunten, 2012).

UV light is electromagnetic radiation with a wavelength of 380 nm–100 nm. UV light at wavelengths around 260 nm, which is the absorption maximum of DNA, is commonly used for disinfection purposes in the treatment of drinking water and waste water (Salgado et al., 2013). In addition to its antimicrobial effects, UV light is also used to degrade organic water components, including micropollutants. It has been shown, that UV light is also able to degrade ADs (Chatzimpaloglou et al., 2021).

In general, when photons are absorbed by a molecule, it is lifted from its energetic ground state into an exited state. There are four ways the molecule can again return to its ground state: Fluorescence and phosphorescence, both of which lead to the emission of a photon, transfer of the energy onto surrounding molecules as heat and chemical transformation, i.e. rearrangement or bond breakage (Bolton and Cotton, 2008). UV lamps that are commonly used for photodegradation are LP-UV lamps, which have a main emission line at $\lambda = 253.7$ nm. Alternatively, medium pressure UV lamps, which have a much broader emission spectrum, can be used (Li et al., 2017).

Elimination efficiencies determined in lab-scale experiments can help when designing fourth treatment stages for WWTPs (Liu et al., 2020). The objective of this study was to determine the degradation efficiency of ozonation and UV-irradiation for the degradation of three ADs, which have been identified as potential priority drugs (Santos et al., 2017; Olalla et al., 2018). To this end, the quantum yields of the photodegradation reactions and the second order reaction rate constants with ozone were determined for CAP, BIC and IRI. Both of these values are independent of the used reactor and can therefore be compared between setups relatively easily. In the context of photodegradation, quantum yields give the number of molecules that are degraded per Einstein of absorbed photons (Bolton and Stefan, 2002). Additionally, the ability of both processes to mineralize the three ADs was determined in mineralization experiments.

2. Materials and methods

2.1. Degradation experiments

2.1.1. Chemicals and stock solutions

CAP and BIC secondary pharmaceutical standards (90–100% purity) as well as uridine (99% purity) were purchased from Sigma-Aldrich (Taufkirchen, Germany) while IRI (98% purity) was purchased from BLD Pharmatech GmbH (Kaiserslautern, Germany). Water and Acetonitrile in HPLC quality and the •OH probe compound 4-chlorobenzoic acid (pCBA) were purchased from VWR International GmbH (Darmstadt, Germany). Ultrapure water (R = 18 MΩ cm) for the degradation experiments was taken from an ELGA Purelab station from Veolia Water Technologies (Celle, Germany). Tert-butanol (t-BuOH, 99% purity) and sodium sulphite (Na_2SO_3, 98% purity) were bought from Merck (Darmstadt, Germany). Ozone was produced using an Anseros Ozomat COM (Tübingen, Germany). For each AD, stock solutions with concentrations of 500 mg L^{-1} and 500 μg L^{-1} in methanol were prepared and stored at −20 °C. 8 mol L^{-1} t-BuOH and 1 mol L^{-1} Na_2SO_3 stock solutions were prepared by dissolving the substance in ultrapure water.

2.1.2. Uridine actinometry

The incident photon flux in the reactor was measured via uridine actinometry according to (von Sonntag and Schuchmann, 1992). A 0.012 mmol L^{-1} solution of uridine was prepared by dissolving 3 mg of uridine in 1 L of ultrapure water. After a 15 min lamp warmup time, this solution was irradiated for 5 min and samples were taken in regular intervals. The uridine concentration inside the samples was measured by spectrophotometer at $\lambda = 262$ nm. The conditions for all experiments are shown in Table 1.

2.1.3. UV degradation and mineralization

All degradation experiments were conducted in a 30 cm high cylindrical glass reactor equipped with a central quartz sleeve and a cooling jacket. The LP-UV lamp used during UV-experiments was a Pen-Ray 3SC-9 from Analytik Jena US (Upland, USA). The outer diameter of the lamp and the quartz sleeve were 9.5 mm and 36 mm respectively and the reactor could hold 390 mL of reaction solution. The pathlength of the light through the reaction solution was 9 mm. A picture of the setup is

shown in Fig. 1.

Cooling water (T = 18 °C) was constantly circulated through the jacket. The reaction solution was mixed by an agitator placed at the bottom of the reactor. The three ADs were individually tested by evaporating the methanol from a set volume of stock solution in a beaker and then dissolving the remaining substance in unbuffered ultrapure water to reach a concentration of 1 μg L^{-1}. pH-values were measured once, at the beginning of the experiment. The irradiation time was 45 min for all three AD solutions. The lamp was turned on 15 min before each experiment to ensure a constant light intensity output. UHPLC-samples were taken in regular intervals and stored at 4 °C until analysis. To ensure that the observed AD degradation is not due to radicals produced from low wavelength UV rays, 20 mmol L^{-1} of t-BuOH were added as radical quencher. All experiments were conducted in triplicate. Dark experiments were done to check for substance loss due to adsorption or hydrolysis and no reduction in concentration was observed. The results of these dark experiments can be found in Fig. S1 of the supplementary information (SI). The molar absorption coefficients were determined from absorptions spectra of a solution of these compounds in water with a known concentration. These absorption spectra are shown in Fig. S2 of the SI.

UV mineralization experiments were conducted using the setup described before but with nominal substance concentrations of 5 mg L^{-1}, degradation times of 120 min and without addition of t-BuOH. In addition to the DOC measurements, the AD's concentration during the DOC experiments was measured by UHPLC-MS/MS after diluting the samples 1:10000.

2.1.4. Ozone degradation and mineralization

Ozone experiments were conducted in the same reactor as UV experiments. Solutions of the ADs were prepared as described in 2.1.3. and pH-values were measured at the beginning of the experiment. An ozone stock solution was prepared by sparging a mixture of ozone and oxygen through ice-cooled ultrapure water. The concentration of the stock solution was determined via the indigo method. For degradation experiments of CAP and IRI an aliquot of the stock was then transferred into the reactor. The reactor setup used for this reaction was the same as for the UV experiments in Fig. 1 but with the lamp turned off.

Since BIC reacted slowly with molecular ozone in our experiments, BIC ozonation experiments were done in the semi-batch setup shown in Fig. 1. The ozone/oxygen mixture was channelled through the reactor constantly at a flow of 20 L h^{-1}. Additionally, experiments with BIC and pCBA were conducted in a semi-batch setup. pCBA reacts slowly with ozone, but quickly with •OH and, using this, the second order rate constant of the reaction of BIC with •OH ($k''_{\bullet OH,BIC}$) was determined. During these experiments, which were again done in triplicate, the concentration of BIC and pCBA were measured using UHPLC-MS/MS and ozone was measured via the indigo-method. $k''_{\bullet OH,BIC}$ was calculated using equations (5)–(7).

Ozone degradation experiments were also conducted with 20 mmol L^{-1} t-BuOH as •OH quencher to determine the reaction rates of the three ADs with molecular ozone. t-BuOH reacts quickly with •OH and terminates the radical chain reaction. Due to the high concentration of t-BuOH, reactions of ADs with •OH were suppressed.

Similar to the UV degradation experiments, UHPLC-MS/MS-samples were taken in regular time intervals and remaining ozone was immediately quenched by 10 μL of 1 mol L^{-1} sodium sulphite solution in the vial. The ozone concentration during every experiment was measured using the indigo-method. All experiments were done in triplicate. The mineralization experiments were conducted in a semi-batch setup at an ozone concentration of 1 mg O_3 per mg of substance. AD concentrations were also measured during the mineralization experiments.

2.2. Kinetic calculations

2.2.1. Photodegradation

The degradation of ADs during the UV irradiation followed pseudo-first order reaction kinetics. The apparent reaction rate constants of the degradation reactions, $k'_{UV,app}$, were determined by plotting the logarithm of the relative concentration of the ADs against the irradiation time:

$$ln\left(\frac{[AD]_t}{[AD]_0}\right) = -k'_{UV,app}t \quad (1)$$

Pseudo-first order rate constants of photochemical reactions in general are specific for the used reactor and cannot be compared between setups. Quantum yields on the other hand are constant for one compound at specific wavelengths and pH values. Quantum yields were calculated using equations (2) and (3) (Sharpless and Linden, 2003; Schwarzenbach et al., 2005, 2003):

$$\varphi = \frac{k'_{UV,app}}{k_s} \quad (2)$$

where φ is the quantum yield for the degradation of the AD during irradiation with a LP-UV lamp (in mol $Einstein^{-1}$),

and

$$k_s = \frac{E_p^0 \varepsilon (1 - 10^{-a \bullet l})}{a \bullet l} \quad (3)$$

with E_p^0 being the incident photon irradiance (in 10^{-3} E s^{-1} cm^{-2}), ε the molar absorption coefficient for the specific AD at 254 nm (in L mol^{-1} cm^{-1}), a the absorbance (in cm^{-1}) and l the length of the path the light takes through the reactor (in cm). k_s (in Einstein mol^{-1} s^{-1}) is the specific rate at which light is absorbed by the AD.

Table 1
Experimental conditions. Ozone degradation experiments with BIC were conducted at higher ozone concentrations due to BIC's low reactivity with molecular ozone.

Experiment	Irradiation intensity [Einstein min^{-1} cm^{-2}]	Target steady state ozone concentration [mg O_3 L^{-1}]	pH-value at start	Tested AD concentra-tion [μg L^{-1}]	Experi-ment duration [min]	Experimental conditions
Uridine actinometry	3.69 •10^{-4}	–		–	5	ultrapure water, 0.012 mmol L^{-1} uridine
UV degradation	3.69 •10^{-4}	–	5.7	1	45	ultrapure water, 20 mM t-BuOH
UV mineralization	3.69 •10^{-4}	–	5.8	5000	120	ultrapure water
Ozone degradation	–	0.15 (CAP and IRI), 1.5 (BIC)	5.7	1	10-15 (CAP and IRI), 120 (BIC)	ultrapure water
Ozone degradation w. t-BuOH	–	0.15 (CAP and IRI), 1.5 (BIC)	5.6	1	10-15 (CAP and IRI), 120 (BIC)	ultrapure water, 20 mM t-BuOH
Ozone degradation w. pCBA (only BIC)	–	1.3	5.7	5	120	ultrapure water, 1 μg L^{-1} pCBA
Ozone mineralization	–	5	5.6	5000	120	ultrapure water

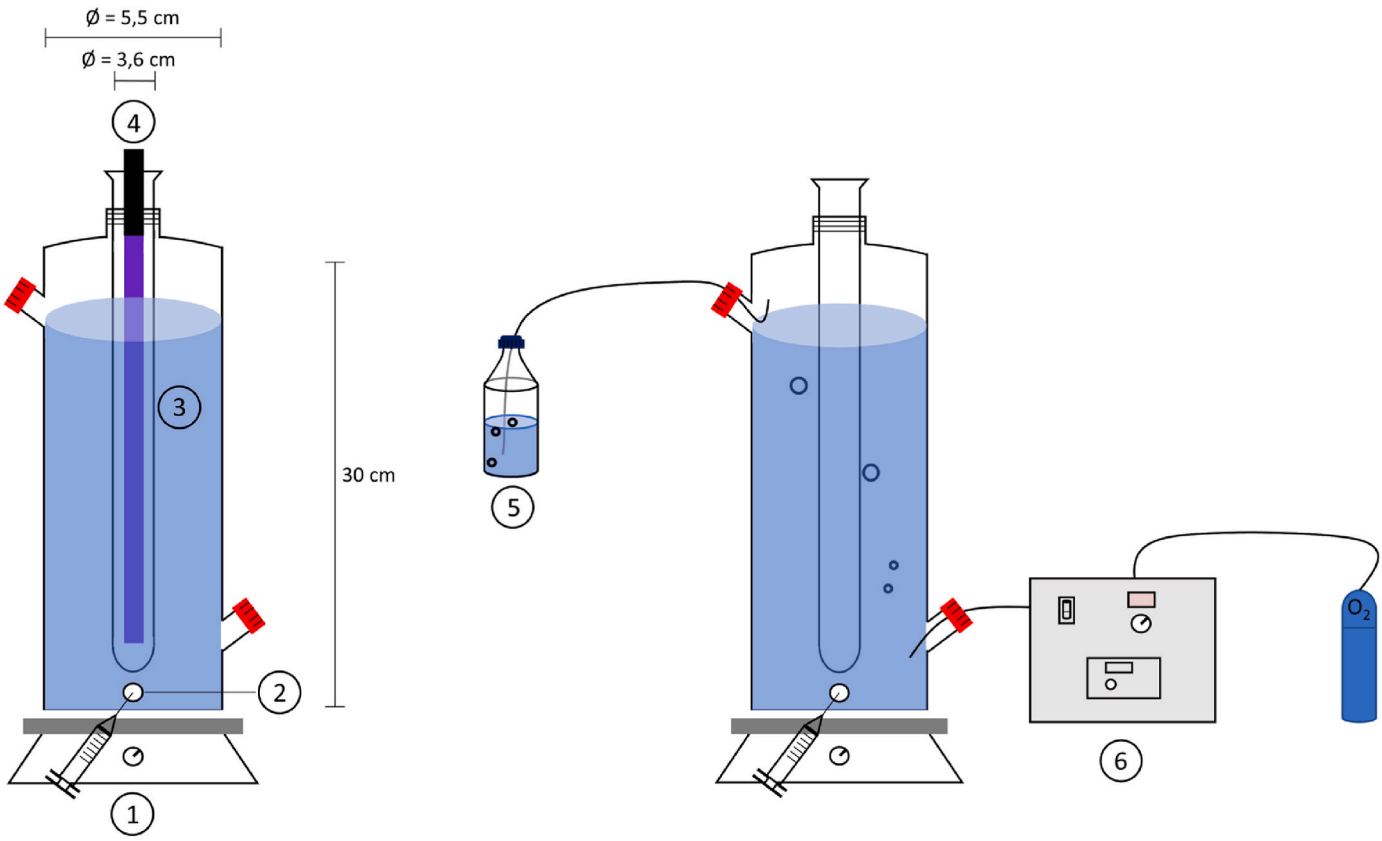

Fig. 1. Reactor setup used in the photodegradation experiments (left) and semi-batch ozonation experiments (right). 1: magnetic stirrer; 2: sampling port; 3: quartz sleeve, 4: LP-UV lamp, 5: bottle for quenching excess ozone, 6: ozone generator. Reactor volume was 390 mL and the reactor was filled with reaction solution through the fitting on the side. Temperature was adjusted via a cooling jacket (not shown).

2.2.2. Degradation by ozone

In all experiments, ozone was added in excess of the ADs (see Table 1). Pseudo-first order reaction rates constants (k'_{O_3}) were calculated using equation (4):

$$ln\left(\frac{[AD]_t}{[AD]_0}\right) = -\, k'_{O_3} t \tag{4}$$

Additionally, the measured ozone concentration was used to calculate the second order reaction rate constant ($k''_{O_3,AD}$) (Dodd et al., 2006; Sonntag and Gunten, 2012):

$$k''_{O_3,AD} = \frac{k'_{O_3}}{c(O_3)} \tag{5}$$

Equations (4) and (5) were used for the calculation of the rate constant with molecular ozone ($k''_{O_3,AD}$) and with both molecular ozone and •OH ($k''_{O_3,AD,app.}$).

2.2.3. Degradation by •OH

$k''_{\bullet OH,BIC}$ was determined using competition kinetics with pCBA as probe compound. pCBA has negligible reactivity with molecular ozone and a rapid reaction with •OH. Therefore, it was assumed that the removal of pCBA in the experiment was caused only by its reaction with •OH and the steady-state concentration of •OH as fraction of the ozone concentration was calculated using the R_{CT}-concept. R_{CT} refers to the ratio of concentration of •OH and ozone and was determined to be constant during a reaction (Elovitz and Gunten, 1999):

$$R_{CT} = \frac{[\bullet OH]}{[O_3]} \tag{6}$$

The rate constant of pCBA with •OH is known at $5 \bullet 10^9$ L mol^{-1} s^{-1} and R_{CT} can therefore be calculated by plotting the logarithm of the relative pCBA concentration at time t against the O_3-exposure using eq. (6) (Elovitz and Gunten, 1999). The O_3-exposure corresponds to the area under the curve of the O_3-concentration:

$$ln\left(\frac{[pCBA]_t}{[pCBA]_0}\right) = k''_{\bullet OH,pCBA} \bullet R_{ct} \int [O_3]dt \tag{7}$$

BIC is degraded by molecular ozone as well as •OH. The removal of BIC can be described by eq. (8) (Garcia-Ac et al., 2010):

$$ln\left(\frac{[BIC]_t}{[BIC]_0}\right) = \left(k''_{\bullet OH,pCBA} \bullet R_{ct} + k''_{O_3,BIC,app}\right) \int [O_3]dt \tag{8}$$

$k''_{O_3,BIC,app}$ is known from prior experiments so the rate constant of BIC with •OH can be calculated from equation (8) (Garcia-Ac et al., 2010).

2.3. Toxicity tests with D. magna

Toxicity tests using *D. magna* were conducted to determine the LC_{50} for partially and fully degraded solutions after treatment by UV and ozone, as well as for the non-degraded substances. The concentration of the original substances before treatment was 1 μg L^{-1}. This concentration was chosen to test the compounds at environmentally relevant conditions. The organisms were cultured and the tests were conducted according to the OECD procedure (OECD, 2004).

2.4. Reagents and analytical methods

ADs and pCBA were quantified with UHPLC-MS/MS using an Agilent 1290 Infinity II-system coupled to an Agilent 6470 triple quadrupole

mass spectrometer with an Agilent Jet Stream electrospray ionisation (ESI) source. The column used was a ZORBAX Eclipse Plus C18 (2.1 × 50 mm, 1.8 μm particle size). Water and acetonitrile with 0.05 % formic acid were used as eluents A and B at a flow rate of 0.3 mL min^{-1}. For each compound, three transitions were detected. The transition with the highest intensity was used for quantification, the other two for qualification. Depending on the compound, positive and negative ionisation modes were used in multiple reaction monitoring (MRM). Additional information about the UHPLC-MS/MS-method can be found in table S1 of the SI.

Ozone in aqueous samples was quantified using the indigo method developed by (Bader, 1982). Indigo concentrations were measured at $\lambda = 600$ nm with a UV1900i spectrophotometer from Shimadzu. For the mineralization experiments, DOC in the water samples was determined by a Shimadzu TOC-L_{CPH} analyser.

3. Results and discussion

3.1. Photodegradation kinetics

During the UV degradation experiments, degradation of 97% of CAP, 90% of BIC and 99% of IRI was achieved within 45 min. In Fig. S3 of the SI, the degradation rates over the course of the experiments can be seen. The degradation curves can be seen in Fig. 2 with the error bars representing the standard deviation of the three experiments at each respective measurement point. The coefficient of determination is > 0.95 for all three graphs. As is clear from Fig. 2, IRI is degraded the fastest, followed by CAP, while BIC is the substance most resistant to degradation by UV. The half-life times of the three compounds range from 6.7 min for IRI to 12.0 min for BIC.

Using the pseudo-first order reaction rate constant from these experiments together with the k_S value from equation (3) and the measured ε, the quantum yield of the degradation reaction was calculated. The values of $k_{UV,app}$ and the quantum yield φ can be found in Table 2. While IRI was degraded the fastest out of the three ADs, CAP actually has the highest quantum yield. This is because the degradation rate not only depends on the quantum yield but also on the number of absorbed photons and therefore the absorbance. The higher absorbance of IRI at $\lambda = 254$ nm compensates for its lower quantum yield and leads to an overall quicker degradation when compared to CAP and BIC.

The quantum yields of six environmentally relevant micropollutants during irradiation with LP-UV lamps at neutral pH-values are also shown in Table 2, alongside the second order rate constants of the reaction with molecular ozone. The ozonation rate constants were determined at pH-values ranging from 5.0 to 7.9, but mostly at neutral pH. Sulfamethoxazole, Ibuprofen and Diclofenac do have quantum yields, which are two

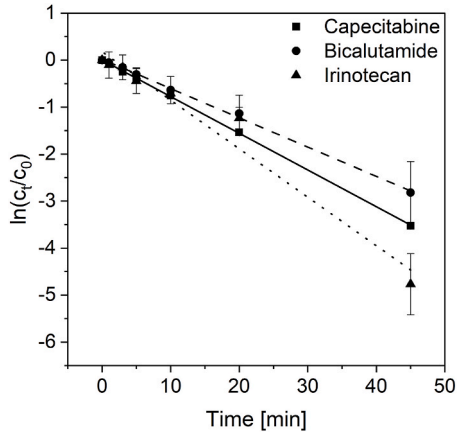

Fig. 2. Photolytic degradation of CAP, BIC and IRI. Initial AD concentration was 1 μg L^{-1}.

to three orders of magnitude higher than the ones determined for the tested compounds. However, Carbamazepine has the lowest quantum yield at $6 \bullet 10^{-4}$ mol $Einstein^{-1}$. Metoprolol and Diatrizoate do have comparable quantum yield to the three ADs.

3.2. Ozonation kinetics

Degradation efficiencies of CAP, BIC and IRI by ozone in ultrapure water were individually tested with substance concentrations of 1 μg L^{-1}. As can be seen in Fig. 3, the degradation of the three ADs in ozonation experiments is best described by pseudo-first order reaction kinetics. The ozone concentrations did not change significantly during the experiment time. The measured ozone concentrations can be found in Table S2. For the ozonation experiments of CAP and IRI, the reaction times for a removal > 95% were below 20 min. The absence of additional organic components in the reaction solution made from ultrapure water means, that ozone can react with no organic molecules expect for the AD, which is present in very low concentration. Additionally, the low pH-value limits the number of •OH that are produced via the reaction of ozone with OH^- and thereby increases ozone stability (Sonntag and Gunten, 2012).

The ozonation experiments with BIC were conducted using a semi-batch setup and the ozone concentration was kept stable by a constant flow of ozone trough the reactor. The first order reaction rate constant of the degradation reaction by ozone in the experiments with (k'_{O_3}) and without t-BuOH ($k'_{O_3,app}$) was determined using eq. (4), second order rate constants ($k''_{O_3,AD}$ and $k''_{O_3,AD,app}$) by equation (5). The results of these experiments are shown in Table 2.

For CAP and IRI the differences between the second order rate constants of the reaction with and without t-BuOH were small ($3.5 \bullet 10^3$ L mol^{-1} s^{-1} and $3.5 \bullet 10^3$ L mol^{-1} s^{-1} for CAP, $1.0 \bullet 10^3$ L mol^{-1} s^{-1} and $1.0 \bullet 10^3$ L mol^{-1} s^{-1} for IRI). The two compounds are readily degraded by molecular ozone, so the degradation reaction is dominated by the direct reaction between the compound and ozone in both experiments. BIC is degraded by ozone mainly via the indirect pathway, so the addition of a radical quencher reduced the already slow reaction speed further from 0.79 L mol^{-1} s^{-1} to 0.1 L mol^{-1} s^{-1}. The slow removal of BIC without the addition of t-BuOH is probably due to the low production of •OH. This is caused by the low concentration of organic substances in the reaction solution and the low pH-value. The rate constant of the reaction of BIC with •OH was calculated to be $2.2 \pm 0.2 \bullet 10^9$ L mol^{-1} s^{-1}. This is a value that was within the expected range of rate constants between micropollutants and •OH (Sudhakaran and Amy, 2013). Other authors reported substantial degradation of BIC during ozonation (Azuma et al., 2019), which might be due to higher concentration of •OH during their experiments. CAP and IRI react quickly with molecular ozone and it was not possible to determine the rate constants of these substances with •OH using the same method.

Typically, ozone reacts quickly with electron-rich moieties. The molecular structures of CAP, BIC and IRI are shown in Fig. S4. Possible sites of attack in CAP are the free electron pairs of secondary and tertiary amines and double bonds. Both of these moieties are present in IRI as well, in addition ozone might react with the aromatic quinoline-ring. BIC is degraded very slowly by ozone due to its relatively electron-deficient amide and sulfone groups. The aromatic rings in BIC are substituted with Fluor and CF_3, respectively, which decreases their electron density and reactivity towards ozone (Sonntag and Gunten, 2012).

Out of the six MPs shown in Table 2, Metoprolol reacts the most comparable to CAP and IRI, while Ibuprofen's rate constant is closest to BIC. Carbamazepine, Diclofenac and Sulfamethoxazole are all degraded faster by ozone than the tested ADs at comparable conditions. As can be seen in Table 2, ozonation is a suitable process to degrade CAP and IRI in water, since the reactivity of these two ADs with molecular ozone is in the range of $1.0 \bullet 10^3$ L mol^{-1} s^{-1}. Therefore, these two compounds

Table 2
Reaction rate parameters of the ADs during UV irradiation and ozonation and quantum yields. Errors represent the standard deviation of values obtained during three experiments. For comparison, ozonation rate constants and quantum yields of five common micropollutants are also shown.

Substance	$k'_{UV,app}$ [min^{-1}]	$t_{1/2,UV}$ [min]	$\varphi_{AD,UV}$ [mol Einstein^{-1}]	$k'_{O_3,AD,app}$ [L $mol^{-1}s^{-1}$]	$k'_{O_3,AD}$ [L $mol^{-1}s^{-1}$]	$k'_{\bullet OH}$ [L $mol^{-1}s^{-1}$]	Sources
CAP	0.078 ± 0.014	8.9	0.012	$3.5 \pm 0.8 \bullet 10^3$	$3.5 \pm 0.3 \bullet 10^3$	–	This study
BIC	0.058 ± 0.017	12.0	0.005	$7.9 \pm 2.1 \bullet 10^{-1}$	$1.0 \pm 0.5 \bullet 10^{-1}$	$2.2 \pm 0.2 \bullet 10^9$	This study
IRI	0.103 ± 0.012	6.7	0.002	$1.0 \pm 0.3 \bullet 10^3$	$1.0 \pm 0.3 \bullet 10^3$	–	This study
Carba-mazepine	–	–	$6 \bullet 10^{-4}$	–	$3.0 \bullet 10^5$	–	(Pereira et al., 2007; McDowell et al., 2005)
Diatrizoate	–	–	0.070	–	1.8	–	(Allard et al., 2016; Ning and Graham, 2008)
Diclofenac	–	–	0.190	–	$1.8 \bullet 10^4$	–	(Keen et al., 2013; Vogna et al., 2004)
Ibuprofen	–	–	0.103	–	9.6	–	(Luo et al., 2018; Huber et al., 2003)
Metoprolol	–	–	0.006	–	$2.0 \bullet 10^3$	–	(Benner et al., 2008; Rivas et al., 2010)
Sulfa-methoxazole	–	–	0.250	–	$4.4 \bullet 10^5$	–	(Hopanna et al., 2020; Dantas et al., 2008)

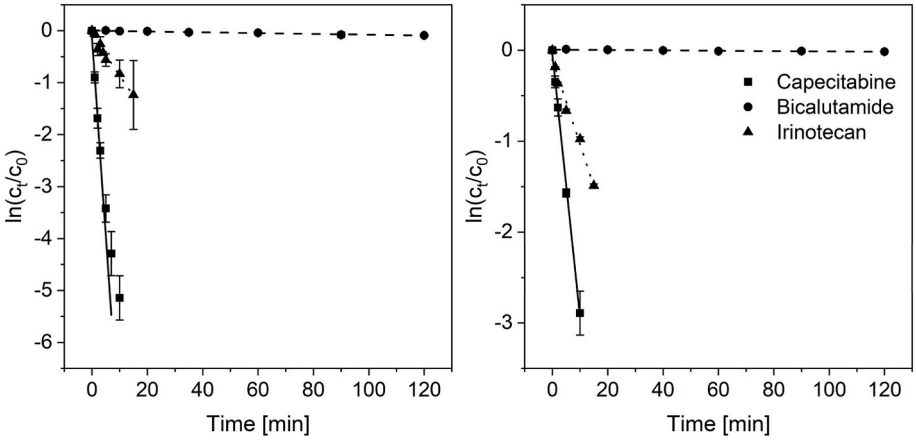

Fig. 3. Ozonation of the three ADs with (right) and without (left) t-BuOH. The initial AD concentration in all experiments was 1 μg L^{-1}.

should be completely eliminated at ozone doses typically applied in waste water treatment (Sonntag and Gunten, 2012). During ozonation, BIC on the other hand is mostly degraded by •OH, resulting in insufficient degradation at standard ozone doses (Garcia-Costa et al., 2022).

Predicted no-effect concentrations (PNEC) are concentrations at which no adverse effect of a substance on the environment is expected (Roman et al., 1999). The PNEC values of CAP, BIC and IRI are 0.077 μg L^{-1}, 10 μg L^{-1} and 0.023 μg L^{-1}, values that are close to, or in the case of IRI even higher, than measured or predicted environmental concentrations (Olalla et al., 2018; Panter et al., 2012; Venâncio et al., 2023). This highlights the need to reduce the input of these ADs into the environment. Of the two tested processes, UV irradiation is able to achieve degradation > 90% of all three ADs, while ozonation can only degrade CAP and IRI at concentrations typical for advanced waste water treatment.

3.3. Mineralization

Mineralization refers to the degradation of organic molecules into inorganic ions, water and CO_2. If only partial degradation is achieved, so called transformation products (TPs) are created. TPs are not necessarily less toxic, which has been shown for TPs of Sulfamethoxazole (Majewsky et al., 2014). It was also shown, that TPs of the anticancer drug cyclophosphamide exhibit a higher toxicity than the drug itself (Lee et al., 2021). That is why a high mineralization rate is generally desired.

Mineralization rates were determined via DOC measurements, which is a common and relatively easy way to measure the degree of mineralization in water samples. The experiments were conducted with a nominal substance concentration of 5 mg L^{-1} so the DOC-concentration could be measured throughout the whole experiment. Linearized relative DOC-concentrations for UV and ozone experiments are shown in Fig. 4. Within 120 min, UV light was able to degrade 80% of the DOC for CAP and IRI and 50% for BIC. Substance concentrations decreased much faster, as can be seen in Fig. S5 and S6. In literature, most authors report low mineralization efficiencies for the irradiation of ADs with UV light alone (e.g. Chatzimpaloglou et al., 2021; Zhang et al., 2017). LP-UV lamps emit radiation mainly at $\lambda = 254$ nm, but radiation at this wavelength is not able to mineralize substantial parts of ADs. Instead, lower wavelength radiation might be responsible for the observed decrease in DOC. In addition to light at $\lambda = 254$ nm, LP-UV lamps also emit photons with a wavelength of 185 nm. At this wavelength, photons are completely absorbed within the first few millimetres after entering the water, but their high energy allows for the production of •OH either via homolysis or photochemical ionisation of water (Zoschke et al., 2014). These radicals are then able to mineralize most organic substances.

Ozone mineralization rates were significantly lower than those observed in the UV experiments. After 120 min, the DOC in the CAP experiment was reduced by 10%, for BIC and IRI the reduction was 30%. Low mineralization rates were expected, as the ozonation process is

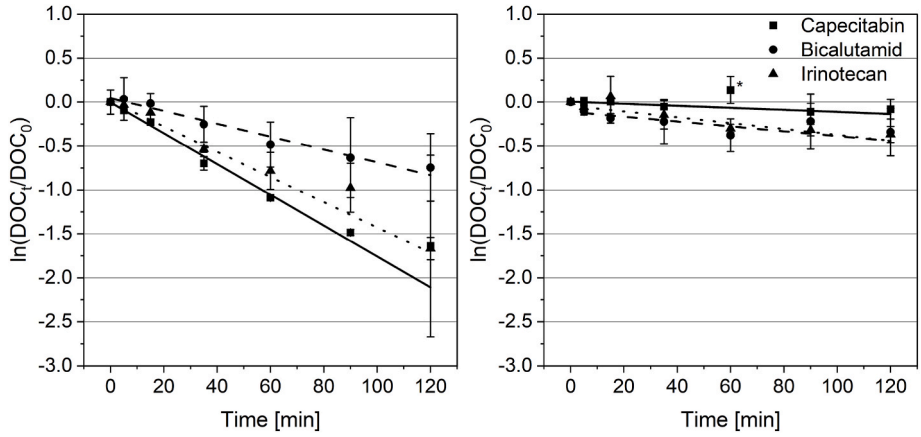

Fig. 4. Linearized DOC-curves for mineralization by UV (left) and ozone (right). *) This value was determined to be an outlier and is not included in the graph.

known for its inability to degrade organic compounds completely. Interestingly, while only a very slow degradation of BIC was observed in the degradation experiments, 30% mineralization were achieved within 120 min, albeit at higher ozone doses (4.3 mg L^{-1} compared to 1.3 mg L^{-1} in the degradation experiments). CAP showed only a low mineralization, despite the high reaction rate constant of the degradation reaction. For the three tested compounds there is no correlation between the speed of the degradation reaction and the mineralization rate. Since both processes degraded the three ADs but did not lead to complete mineralization, newly formed TPs were present in the reaction solutions. To evaluate the toxicity of these TPs, toxicity tests with *D. magna* were conducted. The results can be seen in table S3 in the SI. In short, of the 21 tested solutions only capecitabine degraded by 50 % with ozone showed a decrease in survival. No modifications in immobilization or survival were observed for the other conditions, so their LC_{50} is higher than the tested concentrations of 1 μg L^{-1}. The lack of measured toxicity is probably due to the low concentrations tested and the short exposure duration of the ecotoxicity test. Previous work has shown an EC_{50} (immobilization) between 0.224 and 850 mg L^{-1} in *D. magna* exposed for 48 h to capecitabine (Parrella et al., 2014; Straub, 2010).

Half-lives for DOC during ozonation and UV irradiation are shown in Table 3. Half-lives for the UV-treatment are significantly lower than for ozonation. During both treatments, values for BIC and IRI are similar. Compared to the other two compounds, the half-lives of DOC for CAP are shorter during UV-irradiation and longer during ozonation. Interestingly, there is no correlation between the degradability of one compound and the extent of mineralization. While CAP has the highest $k''_{O_3,AD,app}$, it is mineralized the slowest during ozonation. This can be caused by CAP's TPs, which are possibly more resistant to further degradation by ozone or •OH than the parent compound.

4. Conclusions

In this study we showed that three ADs of potential environmental concern, CAP, BIC and IRI, can be degraded by UV-light. Half-lives between 12.0 min (BIC) and 6.7 min (IRI) have been measured for the three ADs. The quantum yields were calculated to be between 0.002 mol $Einstein^{-1}$ for BIC and 0.012 mol $Einstein^{-1}$ for CAP.

While CAP and IRI were quickly degraded by ozone with second order reaction rate constants $> 10^3$ L mol^{-1} s^{-1}, BIC's reactivity with molecular ozone was low at 0.79 L mol^{-1} s^{-1}. Because of the slow reaction with ozone, the reaction rate constant for the reaction of BIC with •OH, which in this case is the main degradation route, was determined to be 2.15 $\bullet 10^9$ L mol^{-1} s^{-1}. This is the first time the rate constants and quantum yield of BIC are determined. These results showed the suitability of the ozone and UV processes to degrade the three ADs and may help in choosing the most suitable process to degrade the three ADs where this is deemed necessary in water or waste water treatment.

Table 3
Half-lives for the DOC of the three tested ADs during UV-irradiation and ozonation.

	half-live CAP [min]	half-live BIC [min]	half-live IRI [min]
UV	56	75	76
Ozonation	594	274	250

For the UV experiments, mineralization of 80% of the DOC was measured for CAP and IRI and 50% for BIC. Mineralization in the ozone experiments was way lower at 30% (BIC and IRI) and 10% for CAP. The toxicity of partially and fully degraded samples of the treated solutions were tested using *D. magna*. Only one solution showed a significant toxicity. This is probably due to the low concentrations of 1 μg L^{-1} that were used in the assay.

CRediT authorship contribution statement

Stephan Zimmermann: Conceptualization, Formal analysis, Investigation, Validation, Writing – original draft. **Messika Revel:** Conceptualization, Formal analysis, Investigation, Writing – review & editing. **Ewa Borowska:** Conceptualization, Supervision, Writing – review & editing. **Harald Horn:** Resources, Supervision, Writing – review & editing.

Declaration of competing interest

The authors declare that they have no known competing financial interests or personal relationships that could have appeared to influence the work reported in this paper.

Data availability

Data will be made available on request.

Acknowledgements

The study was conducted at the Karlsruhe Institute of Technology (KIT) and the UniLaSalle - Ecole des Métiers de L'Environnement. We would like to thank Rafael Peschke and Matthias Weber for their technical support. Additionally, we would like to thank the Karlsruhe House of Young Scientists (KHYS) for their financial support.

Appendix A. Supplementary data

Supplementary data to this article can be found online at https://doi.

org/10.1016/j.chemosphere.2024.141780.

References

Allard, Sébastien, Criquet, Justine, Prunier, Anaïs, Falantin, Cécilia, Le Person, Annaïg, Tang, Yat-Man, Janet, Croué, Jean-Philippe, 2016. Photodecomposition of iodinated contrast media and subsequent formation of toxic iodinated moieties during final disinfection with chlorinated oxidants. Water Res. 103, 453–461. https://doi.org/10.1016/j.watres.2016.07.050.

Azuma, Takashi, Otomo, Kana, Kunitou, Mari, Shimizu, Mai, Hosomaru, Kaori, Mikata, Shiori, et al., 2019. Removal of pharmaceuticals in water by introduction of ozonated microbubbles. Sep. Purif. Technol. 212, 483–489. https://doi.org/10.1016/j.seppur.2018.11.059.

Bader, H., 1982. Determination of ozone in water by the indigo method: a submitted standard method. Ozone: Sci. Eng. 4 (4), 169–176. https://doi.org/10.1080/01919518208550955.

Benner, Jessica, Salhi, Elisabeth, Ternes, Thomas, Gunten, Urs von, 2008. Ozonation of reverse osmosis concentrate: kinetics and efficiency of beta blocker oxidation. Water Res. 42 (12), 3003–3012. https://doi.org/10.1016/j.watres.2008.04.002.

Besse, Jean-Philippe, Latour, Jean-Francois, Garric, Jeanne, 2012. Anticancer drugs in surface waters: what can we say about the occurrence and environmental significance of cytotoxic, cytostatic and endocrine therapy drugs? Environ. Int. 39 (1), 73–86. https://doi.org/10.1016/j.envint.2011.10.002.

Bolton, James R., Cotton, Christine A., 2008. The Ultraviolet Disinfection Handbook, first ed. American Water Works Association, Denver, CO.

Bolton, James R., Stefan, Mihaela I., 2002. Fundamental photochemical approach to the concepts of fluence (UV dose) and electrical energy efficiency in photochemical degradation reactions. Res. Chem. Intermed. 28 (7–9), 857–870. https://doi.org/10.1163/15685670260469474.

Bray, Freddie, Ferlay, Jacques, Soerjomataram, Isabelle, Siegel, Rebecca L., Torre, Lindsey A., Jemal, Ahmedin, 2018. Global cancer statistics 2018: GLOBOCAN estimates of incidence and mortality worldwide for 36 cancers in 185 countries. CA A Cancer J. Clin. 68 (6), 394–424. https://doi.org/10.3322/caac.21492.

Chatzimpaloglou, A., Christophoridis, C., Fountoulakis, I., Antonopoulou, M., Vlastos, D., Bais, A., Fytianos, K., 2021. Photolytic and photocatalytic degradation of antineoplastic drug irinotecan. Kinetic study, identification of transformation products and toxicity evaluation. Chem. Eng. J. 405, 126866 https://doi.org/10.1016/j.cej.2020.126866.

Dantas, Renato F., Contreras, Sandra, Sans, Carme, Esplugas, Santiago, 2008. Sulfamethoxazole abatement by means of ozonation. J. Hazard Mater. 150 (3), 790–794. https://doi.org/10.1016/j.jhazmat.2007.05.034.

Der Bundesrat, 2023. 100 Kläranlagen müssen aufrüsten – Eawag infotag 2015. www.admin.ch/gov/de/start/dokumentation/medienmitteilungen.msg-id-58567.html, 17.08.2023.

Dodd, Michael C., Buffle, Marc-Olivier, Gunten, Urs von, 2006. Oxidation of antibacterial molecules by aqueous ozone: moiety-specific reaction kinetics and application to ozone-based wastewater treatment. Environ. Sci. Technol. 40 (6), 1969–1977. https://doi.org/10.1021/es051369x.

Elovitz, Michael S., Gunten, Urs von, 1999. Hydroxyl radical/ozone ratios during ozonation processes. I. The R ct concept. Ozone: Sci. Eng. 21 (3), 239–260. https://doi.org/10.1080/01919519908547239.

Garcia-Ac, Araceli, Broséus, Romain, Vincent, Simon, Barbeau, Benoit, Prévost, Michèle, Sauvé, Sébastien, 2010. Oxidation kinetics of cyclophosphamide and methotrexate by ozone in drinking water. Chemosphere 79 (11), 1056–1063. https://doi.org/10.1016/j.chemosphere.2010.03.032.

Garcia-Costa, Alicia L., Alves, Arminda, Madeira, Luís M., Santos, Mónica S.F., 2021. Oxidation processes for cytostatic drugs elimination in aqueous phase: a critical review. J. Environ. Chem. Eng. 9 (1), 104709 https://doi.org/10.1016/j.jece.2020.104709.

Garcia-Costa, Alicia L., Gouveia, Teresa I.A., Pereira, M. Fernando R., Silva, Adrián M.T., Madeira, Luís M., Alves, Arminda, Santos, Mónica S.F., 2022. Intensification strategies for cytostatics degradation by ozone-based processes in aqueous phase. J. Hazard Mater. 440, 129743 https://doi.org/10.1016/j.jhazmat.2022.129743.

Gouveia, Teresa I.A., Silva, Adrián M.T., Ribeiro, Ana R., Alves, Arminda, Santos, Mónica S.F., 2020. Liquid-liquid extraction as a simple tool to quickly quantify fourteen cytostatics in urban wastewaters and access their impact in aquatic biota. Sci. Total Environ. 740, 139995 https://doi.org/10.1016/j.scitotenv.2020.139995.

Hopanna, Mamatha, Mangalgiri, Kiranmayi, Ibitoye, Temitope, Ocasio, Daniel, Snowberger, Sebastian, Blaney, Lee, 2020. Chapter 8 - UV-254 transformation of antibiotics in water and wastewater treatment processes. In: Hernandez-Maldonado, Arturo (Ed.), Contaminants of Emerging Concern in Water and Wastewater. Advanced Treatment Processes. Elsevier Science & Technology, San Diego, pp. 239–297.

Huber, Marc M., Canonica, Silvio, Park, Gun-Young, Gunten, Urs von, 2003. Oxidation of pharmaceuticals during ozonation and advanced oxidation processes. Environ. Sci. Technol. 37 (5), 1016–1024. https://doi.org/10.1021/es025896h.

International Agency for Research on Cancer, 2020. Cancer Tomorrow. https://gco.iarc.fr/tomorrow/en/dataviz/isotype, 02.05.2023.

Keen, Olya S., Thurman, E. Michael, Ferrer, Imma, Dotson, Aaron D., Linden, Karl G., 2013. Dimer formation during UV photolysis of diclofenac. Chemosphere 93 (9), 1948–1956. https://doi.org/10.1016/j.chemosphere.2013.06.079.

Lee, Ji-Young, Lee, Young-Min, Kim, Tae-Kyoung, Choi, Kyungho, Zoh, Kyung-Duk, 2021. Degradation of cyclophosphamide during UV/chlorine reaction: kinetics, byproducts, and their toxicity. Chemosphere 268, 128817. https://doi.org/10.1016/j.chemosphere.2020.128817.

Li, Guo-Qiang, Wang, Wen-Long, Huo, Zheng-Yang, Lu, Yun, Hu, Hong-Ying, 2017. Comparison of UV-LED and low pressure UV for water disinfection: photoreactivation and dark repair of Escherichia coli. Water Res. 126, 134–143. https://doi.org/10.1016/j.watres.2017.09.030.

Liu, Ze, Yang, Yongyuan, Shao, Chenjia, Ji, Zengwen, Wang, Qiaoling, Wang, Shijie, et al., 2020. Ozonation of trace organic compounds in different municipal and industrial wastewaters: kinetic-based prediction of removal efficiency and ozone dose requirements. Chem. Eng. J. 387, 123405 https://doi.org/10.1016/j.cej.2019.123405.

Luo, Shuang, Wei, Zongsu, Spinney, Richard, Zhang, Zulin, Dionysiou, Dionysios D., Gao, Lingwei, et al., 2018. UV direct photolysis of sulfamethoxazole and ibuprofen: an experimental and modelling study. J. Hazard Mater. 343, 132–139. https://doi.org/10.1016/j.jhazmat.2017.09.019.

Majewsky, Marius, Wagner, Danny, Delay, Markus, Bräse, Stefan, Yargeau, Viviane, Horn, Harald, 2014. Antibacterial activity of sulfamethoxazole transformation products (TPs): general relevance for sulfonamide TPs modified at the para position. Chem. Res. Toxicol. 27 (10), 1821–1828. https://doi.org/10.1021/tx500267x.

McDowell, Derek C., Huber, Marc M., Wagner, Manfred, Gunten, Urs von, Ternes, Thomas A., 2005. Ozonation of carbamazepine in drinking water: identification and kinetic study of major oxidation products. Environ. Sci. Technol. 39 (20), 8014–8022. https://doi.org/10.1021/es050043l.

Mišík, Miroslav, Filipic, Metka, Nersesyan, Armen, Kundi, Michael, Isidori, Marina, Knasmueller, Siegfried, 2019. Environmental risk assessment of widely used anticancer drugs (5-fluorouracil, cisplatin, etoposide, imatinib mesylate). Water Res. 164, 114953 https://doi.org/10.1016/j.watres.2019.114953.

Ning, Bo, Graham, Nigel J., 2008. Ozone degradation of iodinated pharmaceutical compounds. J. Environ. Eng. 134 (12), 944–953. https://doi.org/10.1061/(ASCE)0733-9372(2008)134:12(944).

OECD, 2004. Test No. 202: Daphnia sp. acute immobilisation test: OECD. In: OECD Guidelines for the Testing of Chemicals.

Olalla, A., Negreira, N., López de Alda, M., Barceló, D., Valcárcel, Y., 2018. A case study to identify priority cytostatic contaminants in hospital effluents. Chemosphere 190, 417–430. https://doi.org/10.1016/j.chemosphere.2017.09.129.

Panter, G.H., Glennon, Y.C., Robinson, J., Hargreaves, A., Murray-Smith, R., 2012. Effects of the anti-androgen, bicalutamide, in a reduced life-cycle study with the fathead minnow (Pimephales promelas). Aquat. Toxicol. 114–115, 31–38. https://doi.org/10.1016/j.aquatox.2012.02.002.

Parrella, Alfredo; Lavorgna, Margherita; Criscuolo, Emma; Russo, Chiara; Fiumano, Vittorio; Isidori, Marina (2014): Acute and chronic toxicity of six anticancer drugs on rotifers and crustaceans. In: Chemosphere 115, S. 59–66. DOI: 10.1016/j.chemosphere.2014.01.013.

Pereira, Vanessa J., Weinberg, Howard S., Linden, Karl G., Singer, Philip C., 2007. UV degradation kinetics and modeling of pharmaceutical compounds in laboratory grade and surface water via direct and indirect photolysis at 254 nm. Environ. Sci. Technol. 41 (5), 1682–1688. https://doi.org/10.1021/es061491b.

Rivas, F. J.; Gimeno, O.; Borralho, T.; Carbajo, M. (2010): UV-C radiation based methods for aqueous metoprolol elimination. In: J. Hazard. Mater. 179 (1-3), S. 357–362. DOI: 10.1016/j.jhazmat.2010.03.013.

Roman, G., Isnard, P., Jouany, J., 1999. Critical analysis of methods for assessment of predicted no-effect concentration. Ecotoxicol. Environ. Saf. 43 (2), 117–125. https://doi.org/10.1006/eesa.1998.1745.

Salgado, R., Pereira, V.J., Carvalho, G., Soeiro, R., Gaffney, V., Almeida, C., et al., 2013. Photodegradation kinetics and transformation products of ketoprofen, diclofenac and atenolol in pure water and treated wastewater. J. Hazard Mater. 244–245, 516–527. https://doi.org/10.1016/j.jhazmat.2012.10.039.

Santos, Mónica S.F., Franquet-Griell, Helena, Lacorte, Silvia, Madeira, Luis M., Alves, Arminda, 2017. Anticancer drugs in Portuguese surface waters - estimation of concentrations and identification of potentially priority drugs. Chemosphere 184, 1250–1260. https://doi.org/10.1016/j.chemosphere.2017.06.102.

Schwarzenbach, René P., Gschwend, P.M., Imboden, Dieter M., 2005. Environmental Organic Chemistry, second ed. Wiley-Interscience, Hoboken, N.J.

Sharpless, Charles M., Linden, Karl G., 2003. Experimental and model comparisons of low- and medium-pressure Hg lamps for the direct and H2O2 assisted UV photodegradation of N-nitrosodimethylamine in simulated drinking water. Environ. Sci. Technol. 37 (9), 1933–1940. https://doi.org/10.1021/es025814p.

Sonntag, Clemens von, Gunten, Urs von, 2012. Chemistry of ozone in water and wastewater treatment. In: From Basic Principles to Applications. Repr. London, New York.

Straub, Jürg Oliver, 2010. Combined environmental risk assessment for 5-fluorouracil and capecitabine in Europe. Integr. Environ. Assess. Manage 540–566. https://doi.org/10.1897/IEAM_2009-073.1.

Sudhakaran, Sairam, Amy, Gary L., 2013. QSAR models for oxidation of organic micropollutants in water based on ozone and hydroxyl radical rate constants and their chemical classification. Water Res. 47 (3), 1111–1122. https://doi.org/10.1016/j.watres.2012.11.033.

Venâncio, Cátia, Monteiro, Bruna, Lopes, Isabel, Sousa, Ana C.A., 2023. Assessing the risks of capecitabine and its active metabolite 5-fluorouracil to freshwater biota. Environ. Sci. Pollut. Res. 30 (20), 58841–58854. https://doi.org/10.1007/s11356-023-26505-4.

Vogna, Davide, Marotta, Raffaele, Napolitano, Alessandra, Andreozzi, Roberto, d'Ischia, Marco, 2004. Advanced oxidation of the pharmaceutical drug diclofenac with UV/H2O2 and ozone. Water Res. 38 (2), 414–422. https://doi.org/10.1016/j.watres.2003.09.028.

von Sonntag, Clemens, Schuchmann, H.-P., 1992. UV disinfection of drinking water and by-product formation - some basic considerations. J. Water Supply Res. Technol. - Aqua 41, 67–74.

Zhang, Yiqing, Zhang, Jiefeng, Xiao, Yongjun, Chang, Victor W.C., Lim, Teik-Thye, 2017. Direct and indirect photodegradation pathways of cytostatic drugs under UV germicidal irradiation: process kinetics and influences of water matrix species and oxidant dosing. J. Hazard Mater. 324 (Pt B), 481–488. https://doi.org/10.1016/j.jhazmat.2016.11.016.

Zoschke, Kristin, Börnick, Hilmar, Worch, Eckhard, 2014. Vacuum-UV radiation at 185 nm in water treatment–a review. Water Res. 52, 131–145. https://doi.org/10.1016/j.watres.2013.12.034.